

Influenza A Virus Neuraminidase Protein Enhances Cell Survival through Interaction with Carcinoembryonic Antigen-related Cell Adhesion Molecule 6 (CEACAM6) Protein^{*,§}

Received for publication, November 28, 2011, and in revised form, February 22, 2012. Published, JBC Papers in Press, March 6, 2012, DOI 10.1074/jbc.M111.328070

Pratibha Gaur[‡], Priya Ranjan[§], Shipra Sharma[‡], Jenish R. Patel[§], J. Bradford Bowzard[§], Shah K. Rahman[‡], Rashmi Kumari[‡], Shivaprakash Gangappa[§], Jacqueline M. Katz[§], Nancy J. Cox[§], Renu B. Lal[§], Suryaprakash Sambhara[§], and Sunil K. Lal^{‡,1}

From the [‡]Virology Group, International Centre for Genetic Engineering and Biotechnology, Aruna Asaf Ali Road, New Delhi 110067, India and the [§]Influenza Division, National Center for Immunization and Respiratory Diseases, Centers for Disease Control and Prevention, Atlanta, Georgia 30033

Background: The NA protein is required for the release of progeny virions.

Results: The NA/C6 interaction leads to increased tyrosyl phosphorylation of Src, FAK, Akt, GSK3 β , and Bcl-2, which affects cell survival.

Conclusion: A novel role exists for NA in enhancing host cell survival.

Significance: NA not only aids in the release of progeny virions, but also cell survival during viral replication.

The influenza virus neuraminidase (NA) protein primarily aids in the release of progeny virions from infected cells. Here, we demonstrate a novel role for NA in enhancing host cell survival by activating the Src/Akt signaling axis via an interaction with carcinoembryonic antigen-related cell adhesion molecule 6/cluster of differentiation 66c (C6). NA/C6 interaction leads to increased tyrosyl phosphorylation of Src, FAK, Akt, GSK3 β , and Bcl-2, which affects cell survival, proliferation, migration, differentiation, and apoptosis. siRNA-mediated suppression of C6 resulted in a down-regulation of activated Src, FAK, and Akt, increased apoptosis, and reduced expression of viral proteins and viral titers in influenza virus-infected human lung adenocarcinoma epithelial and normal human bronchial epithelial cells. These findings indicate that influenza NA not only aids in the release of progeny virions, but also cell survival during viral replication.

Influenza viruses are human respiratory pathogens that cause both seasonal epidemics and periodic, but unpredictable, pandemics (1). The influenza type A virus genome consists of eight single-stranded negative-sense RNA segments, which encode up to 11 viral proteins. Annual epidemics occur frequently due to antigenic shift, the process by which the major viral surface glycoproteins, hemagglutinin (HA) and neuraminidase (NA),² acquire point mutations allowing the virus to partially overcome preexisting immunity. The less frequent, but

potentially more deadly pandemics occur when a virus with a novel HA and one or more other genes emerges to cause disease and spreads efficiently among humans with little or no preexisting immunity to the novel strain (2).

In addition to their roles in entry, genome mRNA synthesis, assembly, and budding, many influenza viral proteins also have secondary functions that alter the cellular environment to permit viral replication. For example, the nonstructural protein 1 (NS1) of influenza virus has been reported to activate the phosphatidylinositol 3-kinase (PI3K)/Akt pathway, which suppresses apoptosis (3–5), whereas overexpression of the nucleoprotein (NP) and matrix 1 (M1) protein was shown to activate NF- κ B (6). Likewise, binding of recombinant HA to cell receptors induces protein kinase C signaling, and the overexpression of HA activates NF- κ B (7, 8). The NA protein is critical for virus assembly, budding, and release from the infected cell (9) and activates TGF- β to contribute to apoptosis (10). NA activity has also been associated with the ability to induce type I interferon in a strain-dependent manner (11), and treatment of cells with purified NA was shown to stimulate the expression of TNF- α (12).

In the present study, we show that influenza NA interacts with human carcinoembryonic antigen-related cell adhesion molecule 6/cluster of differentiation 66c (CEACAM6/CD66c, or C6), a glycosylphosphatidylinositol-linked Ig-like membrane protein. Overexpression of C6 causes resistance to anoikis (13), a form of cell death, and activated c-Src signaling in a caveolin-1-dependent manner (14). Inhibition of C6 expression using siRNA led to a loss of activation of Src, FAK, and Akt, increased cell death, and a significant loss of expression of viral proteins. These findings propose a novel role for the NA protein in sustaining cell survival for enhanced viral replication.

EXPERIMENTAL PROCEDURES

Plasmid Constructs, Antibodies, siRNA, Virus Strains, and Mammalian Cell Lines—For mammalian expression, NA was cloned into pXJ41neo (Dr. Yee-Joo Tan, National University of Singapore). The full-length human C6 gene cloned into the

* This work was supported by internal funds from the International Centre for Genetic Engineering and Biotechnology (ICGEB), New Delhi, a research grant from the Department of Biotechnology, India (to S. K. L.), and a training and research grant from the Centers for Disease Control (CDC), Atlanta (to S. K. L.).

§ This article contains supplemental Figs. S1–S4.

¹ To whom correspondence should be addressed. Tel.: 91-9818522900; Fax: 91-11-26742316; E-mail: sunillal@icgeb.res.in.

² The abbreviations used are: NA, neuraminidase; C6, CEACAM6/CD66c; CD66c, cluster of differentiation 66c; CEACAM6, carcinoembryonic antigen-related cell adhesion molecule 6; m.o.i., multiplicity of infection; NHBE, normal human bronchial epithelial; NP, nucleoprotein; NS1, nonstructural protein 1; TPCK, L-1-tosylamido-2-phenylethyl chloromethyl ketone.

TABLE 1
C6-specific siRNA sequences

GAUCACAGUCUCUGGAAGU
GAACAUGGCUAAAUACAACU
GAGGGUAAACUUAACAGAGU
CUACAUAUCUCCACUGAAA

pRc/CMV plasmid was a kind gift from Wolfgang Zimmermann (Tumor Immunology Laboratory Life Center, University Clinic-Grosshadern Muenchen, Germany). Anti-NA antibody was purchased from Meridian Life Sciences (Saco, ME), and anti-C6 and anti-HA tag antibodies were purchased from Santa Cruz Biotechnology (Santa Cruz, CA). Antibodies against FAK, P-Y925-FAK, Akt, P-Akt, P-GSK3 β , P-Bcl-2, Bcl-2, and P-Src were obtained from Cell Signaling Technology (Danvers, MA). Anti- β -actin antibody was purchased from Sigma-Aldrich. A pool of siRNAs specific for C6, Akt1 (L-003000), Akt2 (L-003001), and Akt3 (L-003002) was purchased from Dharmacon (Lafayette, CO), and the sequences are listed in Table 1. For virus infection experiments, the A/Puerto Rico/8/34 (PR8) influenza virus strain was used at a multiplicity of infection (m.o.i.) of 1 unless specified otherwise. An 3-(4,5-dimethylthiazol-2-yl)-2,5-diphenyltetrazolium bromide (MTT) assay kit from Biotium (Hayward, CA) and an Annexin-V kit (BD Biosciences) were used for measuring cell growth and apoptosis, respectively. Other influenza virus strains used in the co-immunoprecipitation experiments are listed in Fig. 1F. Human embryonic kidney 293 (HEK-293) and human lung adenocarcinoma epithelial (A549) cell lines were purchased from ATCC. Normal human bronchial epithelial (NHBE) cells (Lonza, Switzerland) were maintained as specified by the supplier. Akt activator YS-49 was purchased from Sigma. Akt inhibitors GSK 690693 was purchased from Tocris Bioscience, MN. Akt inhibitors Triciribine and 124005 were purchased from EMD Millipore.

Yeast Two-hybrid Screening—Hybrid Hunter (Invitrogen) yeast two-hybrid system was used for screening. The A/Chick-en/Hatay/2004 NA gene (H5N1) cloned in the pHybLex/Zeo vector was used as a bait to screen a human lung cDNA library cloned in pYESTrp2 vector. The L40 strain of *Saccharomyces cerevisiae* was used as host for co-transformation of bait and library plasmids. Colonies that grew on T⁺H⁺/L⁺ Zeo⁺ (standard dextrose plates with zeocine but lacking leucine tryptophan and histidine) medium supplemented with 10 mM aminotriazole were considered as initial positives. β -Galactosidase assays were performed as described in the Invitrogen manual (15, 16) as an additional evidence for determining the strength of interaction.

In Vitro Translation and Western Blot Analysis—*In vitro* transcription/translation was performed using the TNT T7 kit from Promega according to the manufacturer's recommendations. For Western blotting, cells were treated with lysis buffer (20 mM HEPES, pH 7.5, 150 mM NaCl, 1 mM EDTA, 0.1% Triton X-100) supplemented with Complete protease-inhibitor mixture (Roche Diagnostics), and the lysates were subjected to SDS-PAGE. Proteins were transferred to nitrocellulose and probed with the indicated antibodies.

Co-immunoprecipitation—Cells were harvested in radioimmunoprecipitation assay buffer (Sigma-Aldrich), and cell

lysates were incubated with primary antibody overnight followed by incubation with protein A Dynabeads (Invitrogen) for 2 h. The beads were washed three times with PBS, suspended in Laemmli buffer (62.5 mM Tris-HCl, pH 6.8, 25% glycerol, 2% SDS, 0.01% bromophenol blue), boiled for 10 min, and spun down. Supernatants were collected and analyzed by Western blotting.

Immunofluorescence Microscopy—A549 cells infected with PR8 influenza virus at a m.o.i. of 1 were fixed at different time points in PBS with 2% paraformaldehyde for 30 min, permeabilized with 0.5% Triton X-100 for 5 min at room temperature, and blocked with PBS containing 2% BSA. Immunostaining was performed using mouse anti-C6 and rabbit anti-NA antibodies. Unbound antibodies were washed away with PBS, and cells were incubated with goat anti-rabbit Alexa Fluor 488 antibodies and goat anti-mouse Alexa Fluor 594 conjugated antibodies. Nuclei were stained with DAPI. Images were captured using a Leica DM6000 CFS Confocal Microscope.

Quantification of C6 and NP mRNA by Real-time RT-PCR—Total RNA from cells was extracted using the RNeasy Mini Kit (Qiagen) and treated with DNase I (Invitrogen). Two μ g of RNA was reverse-transcribed using the ThermoScript RT (Invitrogen) in a volume of 20 μ l. Resulting cDNA was diluted 1:10 and 2.5 μ l was used in a SYBR Green (SA Biosciences, Frederick, MD)-based real-time PCR in a volume of 25 μ l using a Mx3000 real-time PCR instrument (Stratagene). Primers used for real-time RT-PCR were: C6 forward, GTTGTGCTGGAGATGGAGG; C6 reverse, ACGTCACCCAGAATGACACA. Primer sets specific for an internal control β -actin, ACCAACTGGGACGACATGGAGAAA (forward) and TAGCACAGCCTGGATAGCAACGTA (reverse) and NP gene, CTCGTCGCTTATGACAAAGAAG (forward) and AGATCATCATGTGAGTCAGAC (reverse) were used for real-time PCR ($\Delta\Delta$ Ct method) and -fold changes were calculated by comparing with the uninfected samples. These experiments were performed at least three times with similar results.

Virus Infection, C6, and Akt Silencing—Scrambled and transcript-specific siRNAs specific for human C6 (Table 1) and Akt1, Akt2, and Akt3 were transfected into A549 and NHBE cells using Dharmafect1 siRNA transfection reagent. Cells were plated at a density of 10⁶/well in a 6-well plate and transfected with a 50 nM concentration of each of the indicated siRNAs 24 h prior to infection with A/PR/8/34. One day later, cells were harvested, and lysates were analyzed for NS1, NP, FAK, P-FAK, Akt, P-Akt, P-GSK3 β , P-Bcl-2, and Bcl-2, P-Src, and β -actin using Western blotting.

Plaque Assay—Madin-Darby canine kidney cells were seeded in 6-well plates (\sim 10⁶ cells/well), and the plates were incubated at 37 °C overnight. Cell monolayers in all 6-well plates were washed twice with DMEM, and the supernatant-containing virus was added in a volume of 200 μ l at different dilutions. Each dilution was plated in duplicate. Plates were incubated with virus for 1 h, followed by washing with DMEM with 0.3% BSA. The cells were overlaid with 1.6% agarose (Invitrogen), in L15 medium (2 \times L15, 1 M HEPES, 200 mM glutamine, 50 μ g/ml gentamycin, NaHCO₃, and penicillin-streptomycin) with 1 μ g/ml TPCK-treated trypsin (Sigma-Aldrich). We placed the plates in an incubator for 2–3 days, carefully removed the aga-

rose, and fixed the cells with 70% ethanol for 5–10 min. Later, we stained them with crystal violet for 30 min.

MTT Assay—A549 and NHBE cells were seeded at 10,000 cells/well in a 96-well dish. After adherence, they were treated with either scrambled or C6-specific siRNAs and infected with influenza virus 24 h later. Ten μ l of MTT solution/well was added and incubated at 37 °C for 4 h to allow for the formation of formazan. The medium was removed, and 200 μ l DMSO was added to each well to dissolve the formazan. Absorbance was measured on an ELISA plate reader with a test wavelength of 570 nm and a reference wavelength of 630 nm to obtain sample signal ($A_{570} - A_{630}$). DMSO was used as a reference.

Flow Cytometric Analysis for Annexin-V Cell Death Assay—A549 cells were transfected with scrambled and C6-specific siRNA and infected with influenza virus 24 h later, as described above. Cells were harvested using 0.05% trypsin/EDTA (Invitrogen) and washed twice with cold 1 \times PBS (Invitrogen). 200,000 cells were added per well in a 96-well round-bottom plate (Corning, Corning, NY) and stained with 5 μ l of Annexin-V FITC (BD Biosciences) in 100 μ l of 1 \times Annexin-V binding buffer for 15 min at room temperature. Samples were diluted 1:5 and analyzed using a FACS Calibur flow cytometer (BD Biosciences) and Flowjo software (Treestar, Ashland, OR).

RESULTS

Conserved Interaction of NA with C6 among Different Subtypes of Influenza Virus—To identify new cellular binding partners for the influenza virus NA protein, a mammalian lung cDNA library was screened using the NA gene from a highly pathogenic avian influenza virus as a bait, A/Chicken/Hatay/2004, in a yeast two-hybrid assay (supplemental Fig. S1A). Potential positive colonies were confirmed using β -galactosidase assays (supplemental Fig. S1B), and the inserts in these plasmids were sequenced. BLAST analysis identified the insert as the mammalian C6 cDNA (supplemental Fig. S1C). To confirm the NA/C6 interaction, both proteins were expressed using an *in vitro* coupled transcription-translation rabbit reticulocyte system in the presence of [35 S]Met (Fig. 1A). Immunoprecipitation of these reactions showed that NA co-precipitated with C6 and vice versa (Fig. 1A, lane 2). Furthermore, immunofluorescence analysis, following co-transfection of HEK-293 cells, which do not express endogenous C6, with NA and C6 expression plasmids revealed a co-localization of both proteins to the plasma membrane (Fig. 1B). Thus, NA co-localizes and interacts with C6.

To determine whether such an interaction also occurs during viral infection, A549 cells were infected at an m.o.i. of 1 with a laboratory-adapted influenza virus, A/Puerto Rico/8/34 (H1N1; PR8). After 24 h, lysates were harvested, and NA and C6 proteins were immunoprecipitated using specific antibodies. The NA of PR8 was found to co-precipitate with C6; and conversely, C6 was co-precipitated with NA (Fig. 1C, panels 1 and 2, respectively). Immunoprecipitation of each antigen alone (Fig. 1C, panels 3 and 4) and Western blotting of total cell lysates (Fig. 1C, panels 6 and 7) also shown the expression of these proteins. In similar experiments, A549 and NHBE cells were infected with other influenza virus subtypes (Fig. 1, D and E), including a reassortant H3N2 (A/X-31), a neurotropic

H1N1 (A/WSN/1933), and a recently emerged pandemic H1N1 (A/California/08/2009). The NA/C6 interaction was conserved among all virus strains (Fig. 1F). Furthermore, co-localization of NA and C6 in A549 cells infected with PR8 by immunofluorescence indicates that this interaction is also likely to occur within infected cells (Fig. 2).

Influenza Infection Increases C6 mRNA and Protein Expression, and Knocking Down C6 Down-regulates Viral Protein Expression—To test whether influenza virus infection alters C6 expression levels, we infected A549 cells with PR8 (m.o.i. = 1) and extracted RNA and proteins at various times after infection. Quantitative real-time PCR analyses indicated a low constitutive level of C6 mRNA expression in A549 cells which was increased after viral infection (Fig. 3Aa). These mRNA levels corresponded to comparable increase in C6 protein expression as indicated by Western blot analyses (Fig. 3Ab). We next determined the effect of different doses of virus on the enhancement of C6 expression. A549 cells were infected with PR8 at three different m.o.i.s (0.1, 0.5, and 5) for 24 h, and C6 mRNA (Fig. 3Ba) and protein (Fig. 3Bb) levels were quantified. Here, NP was used as a control for mRNA and protein expression (Fig. 3, A, c and d; and B, c and d). C6 expression was induced in virus-infected A549 cells in a PR8 dose-dependent manner.

To determine whether the increase in C6 protein affects viral replication, C6 expression in A549 cells was abrogated using siRNA prior to infection with PR8. In addition to knocking down C6 mRNA and protein levels, the siRNA (Table 1) also substantially down-regulated the mRNA and protein levels of NS1 and NP (Fig. 4). In contrast, a negative control scrambled siRNA did not affect the levels of C6 or either viral protein. Furthermore, there was significant reduction in viral titer (~ 1 log) in cells treated with C6 siRNA and subsequently infected with PR8 in contrast to those treated with scrambled siRNA and infected with PR8 virus (supplemental Fig. S2B). Altogether, these results clearly suggest that the decrease in C6 observed upon viral infection is necessary for an efficient production of viral proteins and responsible for viral replication.

NA Activates Akt Cell Survival Pathway through Its Interaction with C6—Given the role of C6 in cell survival pathways (14, 17, 18), we hypothesized that the interaction of NA with C6 could lead to the activation of Akt-mediated cell survival (5). To address this, we transfected HEK-293 cells with influenza NA and human C6 expression vectors or with C6 and vector-only control plasmids. Cell lysates prepared 48 h after transfection were subject to Western blot analyses using antibodies specific for phospho-Src (Tyr-416), phospho-FAK (Tyr-925), phospho-ERK (Tyr-204), and phospho-Akt (Thr-308). As shown in Fig. 5A, phosphorylation of Src, FAK, and Akt was stimulated in NA and C6 co-transfected cells relative to the controls. However, phosphorylation of ERK was unaffected. In A549 cells, expression of NA alone was sufficient to induce phosphorylation of Src, FAK, and Akt compared with the vector-only control (Fig. 5B). The densitometry graphs compare the relative intensity of the bands (Fig. 5, A and B, respectively). These results suggest that the NA/C6 interaction activates the cell survival signaling pathway through Akt.

To ascertain further the importance of C6 in the activation of the Akt cell survival pathway, we used siRNA to inhibit C6

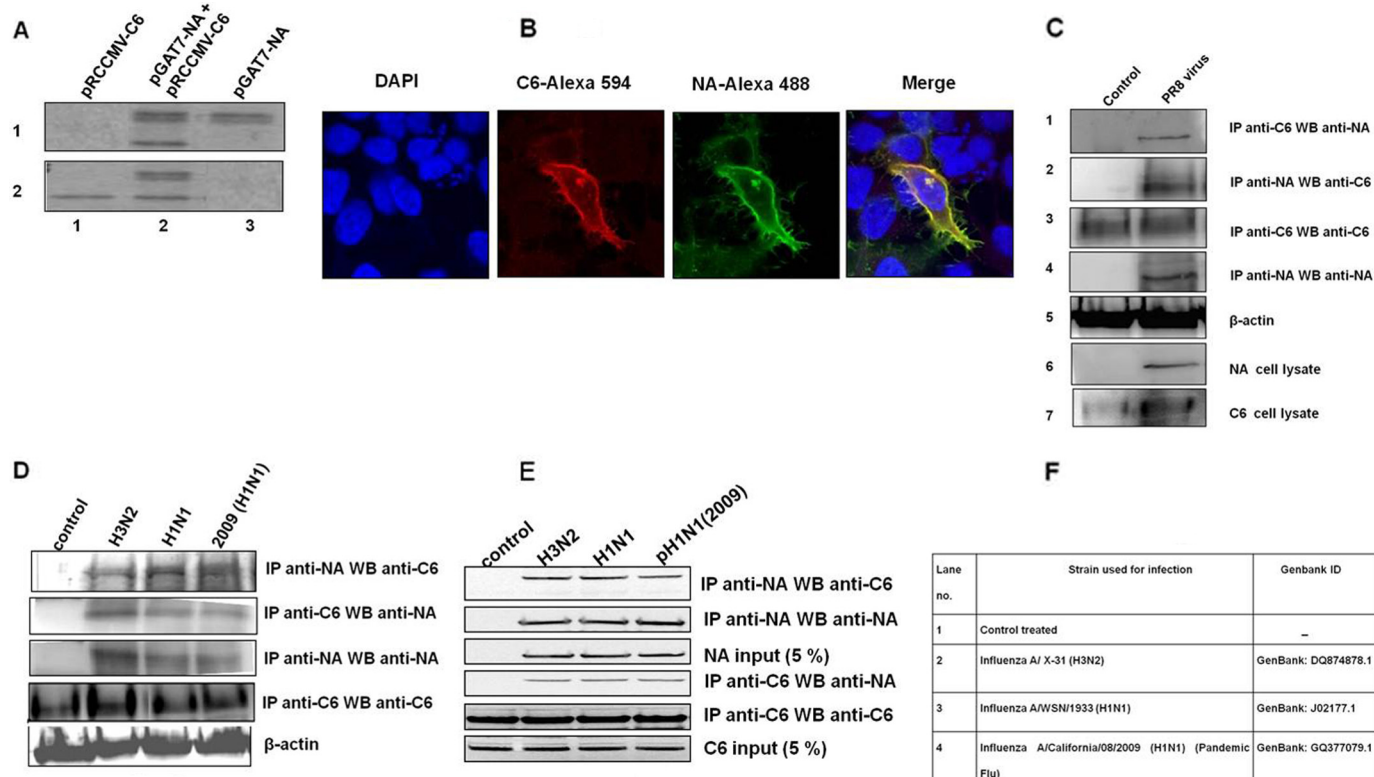


FIGURE 1. Influenza A virus NA interacts with host protein C6. *A*, *in vitro* co-immunoprecipitation of NA and C6. HA-tagged NA and untagged C6 were translated *in vitro* in the presence of [³⁵S]methionine and immunoprecipitated with α -HA or α -C6 antibodies, respectively. Complexes were subjected to 12% SDS-PAGE followed by autoradiography. NA co-immunoprecipitated with C6 pulled down by C6-specific antibody (*panel 2, lane 2*). Similarly, C6 co-immunoprecipitated with NA protein pulled down by α -HA antibody (*panel 1, lane 2*). *B*, NA co-localization with C6 in HEK-293 cells. NA and C6 expression plasmids were transfected into HEK-293 cells. 48 h after transfection, cells were fixed, and nuclei were stained with DAPI (*blue*). C6 was labeled with goat anti-mouse Alexa Fluor 594 (*red*), and NA was labeled with goat anti-rabbit Alexa Fluor 488 (*green*) antibody. The *rightmost panel* shows that 48 h after transfection NA and C6 co-localize on the cell membrane. *C*, co-immunoprecipitation of NA with C6 in PR8 virus-infected cells. C6 is endogenously present in A549 cells. A549 cells were infected with A/PR8/34 influenza viruses at a m.o.i. of 1 and harvested at 24 h after infection. Co-immunoprecipitation and Western blot analysis were done using NA- and C6-specific antibodies. *Lane 1* shows uninfected A549 cells, and *lane 2* shows interaction between NA and C6 in PR8-infected cells. *D*, co-immunoprecipitations of NA and C6 in different subtypes of influenza virus. A549 cells were infected with different subtypes of influenza virus at a m.o.i. of 1 and harvested at 24 h after infection. Co-immunoprecipitation and Western blot analysis were conducted using NA- and C6-specific antibodies. *Lane 1* shows uninfected A549 cells, *lane 2-4* show interactions between C6 and NA from A/X-31H3N2, A/WSN/1933, H1N1, and A/California/08/2009 H1N1 subtypes, respectively. *E*, co-immunoprecipitation of NA and C6 in primary cells infected with different subtypes of influenza viruses. NHBE cells were transfected with C6 expression vectors or control vectors. 24 h after transfection, cells were infected with different subtypes of influenza viruses at a m.o.i. of 1 and harvested after 24 h. Co-immunoprecipitation and Western blot analysis were conducted using NA- and C6-specific antibodies. *Lane 1* shows uninfected NHBE cells, *lane 2-4* show interactions between C6 and NA from A/X-31(H3N2), A/WSN/1933 (H1N1), and A/California/08/2009 (pH1N1) viruses, respectively. *F*, various influenza virus strains used for this study.

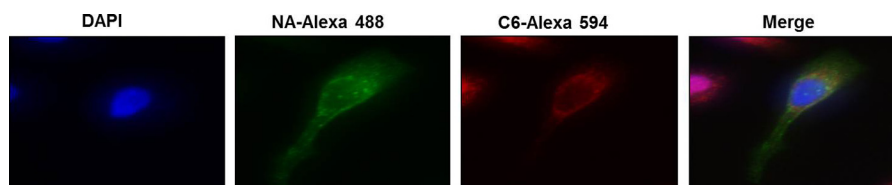


FIGURE 2. NA and C6 co-localize on the membrane of mammalian cells (A549) infected with PR8 influenza A virus. A549 cells were infected with PR8 influenza virus at a m.o.i. of 1 and fixed at 16 h after infection. Nuclei were stained with DAPI (*blue*). NA was labeled with goat anti-rabbit Alexa Fluor 488 (*green*) antibody, and C6 was labeled with goat anti-mouse Alexa Fluor 594 (*red*) antibody. Protein localization was visualized by confocal microscopy.

expression in A549 and NHBE cells. As expected, infection with PR8 virus resulted in enhanced phosphorylation of Src, FAK, and Akt (Fig. 5, *C* and *D*; densitometric analysis shown in Fig. 5C). In contrast, infection of cells after C6-specific siRNA treatment resulted in a substantial suppression in phosphorylation of Src, FAK, Akt, and Bcl-2 molecules in both A549 (Fig. 5C) and NHBE cells (Fig. 5D). Total levels of each of these proteins were unaffected by virus infection. These data demonstrate a critical role for C6 in virus-induced activation of Akt.

We next studied the biological effect of the NA-C6 complex on cell survival using an MTT assay. A549 and NHBE cells transfected with scrambled siRNA and C6-specific siRNA were infected with PR8 virus and then subjected to MTT assay. Substantial cell death was observed in C6 siRNA-treated cells compared with the scrambled controls (~ 67 and $\sim 50\%$ relative viability, respectively, Fig. 6, *A* and *B*). Staining for Annexin-V, a marker for the early stages of cell death, also indicated that viability was decreased upon inhibition of C6 in A549 cells (Fig.

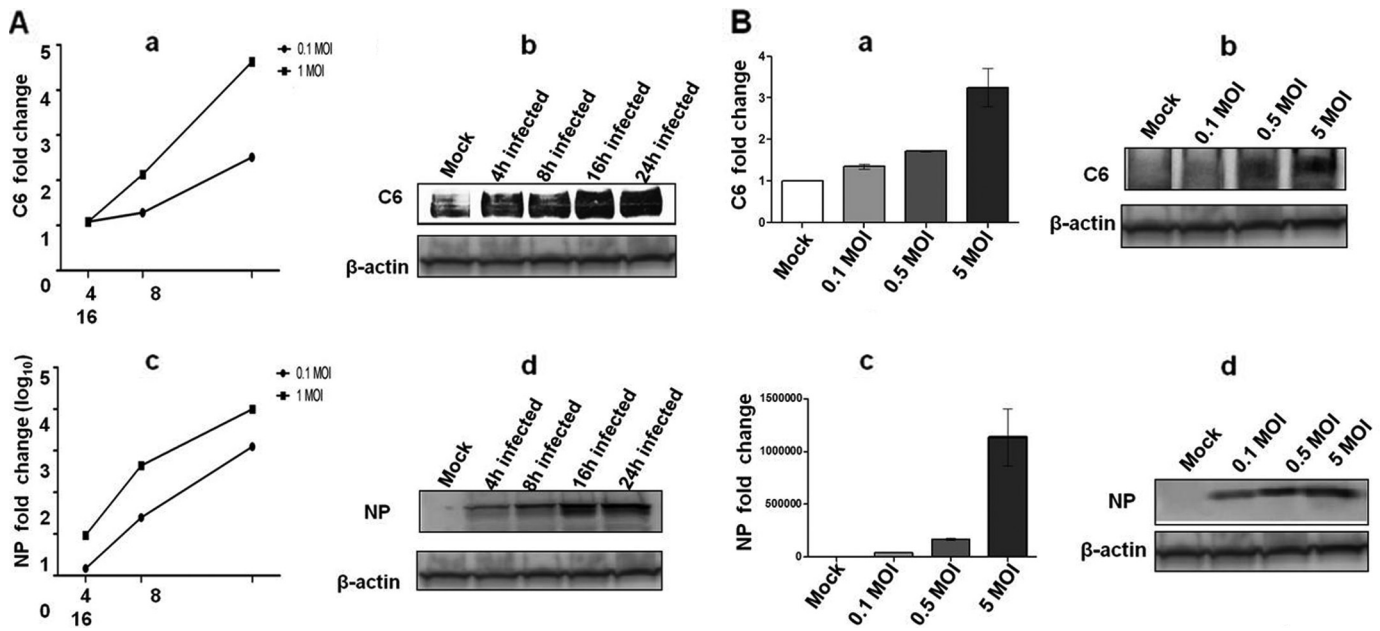


FIGURE 3. Influenza infection elevates C6 mRNA and protein expression levels in a time- and dose-dependent manner. A549 cells were infected with PR8 influenza virus at a m.o.i. of 1 and harvested 24 h after infection. *A*, real-time PCR or Western blot analysis of C6 (*a* and *b*) and NP (*c* and *d*). Expression increases with time of PR8 infection (4, 6, and 16 h at m.o.i. of 0.1 and 1.0). *B*, real-time PCR analysis ($n = 2$) of C6 (*a*) and NP (*c*) expression increases with increasing dose of PR8 infection (m.o.i. of 0.1, 0.5, and 5.0); the same samples were checked for protein expression of C6 (*b*) and NP (*d*).

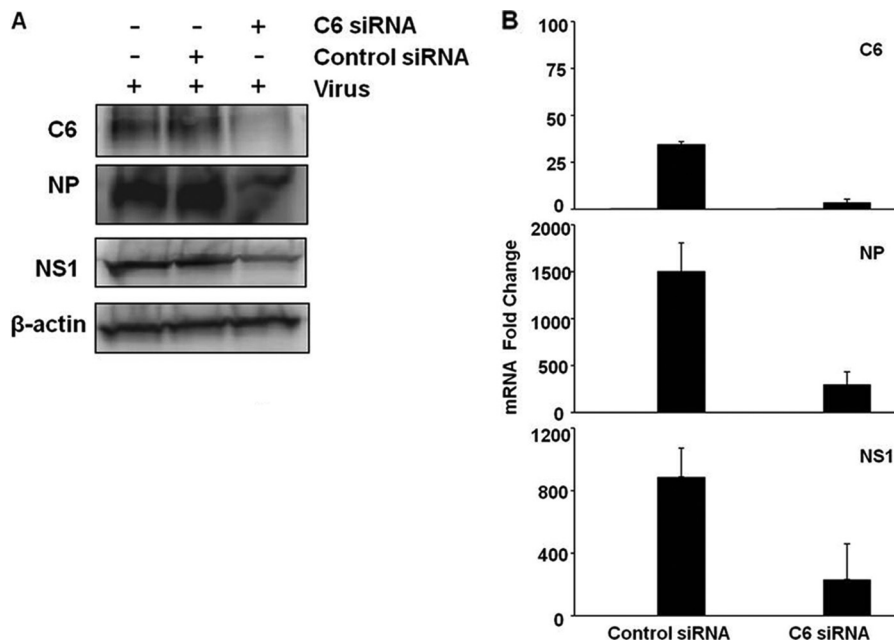


FIGURE 4. C6 siRNA-treated influenza A virus-infected cells down-regulate NP and NS1. *A*, A549 cells were treated with siRNA against C6 and scrambled siRNA for 48 h and then infected with PR8 virus at an m.o.i. of 1. Cells were harvested at 24 h after infection, and equal amounts of protein from control and treated cell extracts were subjected to Western blot analysis. *First lane* shows control levels of C6, NP, and NS1. *Second lane* shows minimal effect of scrambled siRNA on the same protein levels. *Third lane in top panel* shows down-regulated levels of C6. *Third lane in second panel from top* shows down-regulation of NP after using siRNA against C6. *Third lane in second panel from bottom* shows down-regulation of NS1 after using siRNA against C6. *Bottom panel* shows β -actin loading control. *B*, NHBE cells were treated with siRNA against C6 and control siRNA for 24 h and then infected with PR8 virus at m.o.i. of 1. Cells were harvested at 24 h after infection and analyzed for mRNA expression of C6, NP, and NS1 by quantitative real-time PCR.

6C). We have also checked the C6 siRNA effect on cell growth and viability in uninfected samples (supplemental Fig. S2A). There was a significant decrease in cell viability with the knock-down of C6 and virus-infected samples in contrast to their control.

Data shown above clearly indicate NA overexpression and its interaction with C6-increased Akt phosphorylation. To inves-

tigate the role of Akt phosphorylation in influenza virus infection, A549 and NHBE cells were treated with PI3K inhibitors (LY294002 and wortmanin), Akt activator, YS-49 or Akt inhibitors, Triciribine, 124005, or GSK690693 followed by infection with PR8 virus at a m.o.i. of 1. The samples were analyzed by Western blotting to check the phosphorylation of Akt (Fig. 7, *Aa* and *Ba*). It was clearly evident that phosphorylation levels

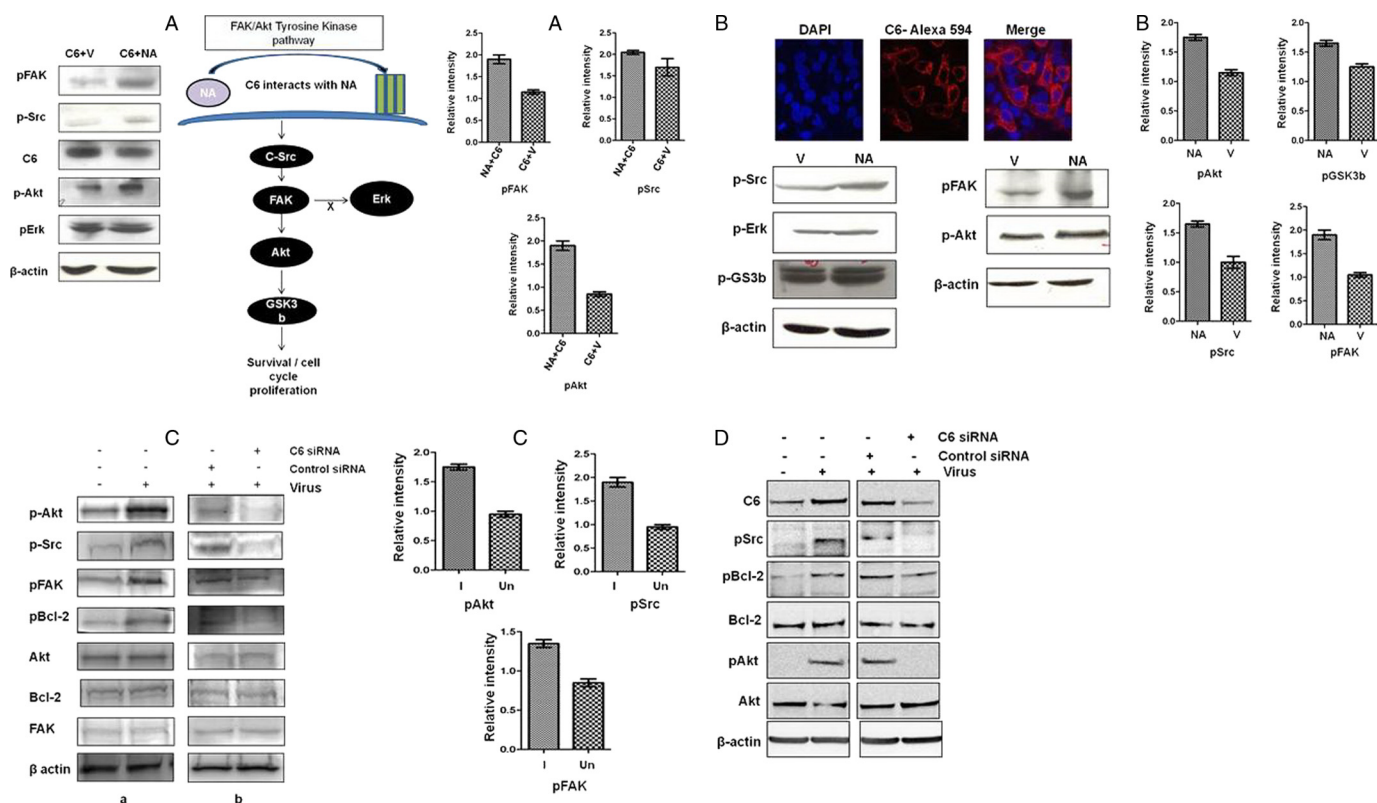


FIGURE 5. NA expression in mammalian cells leads to up-regulation of FAK and Akt phosphorylation. HEK-293 and A549 cells were transfected with the plasmid expressing H5N1 NA or empty plasmid (pcDNA 3.1 myc/his) as control and harvested at 48 h after transfection. Equal amounts of protein from test and control sets were subjected to Western blot analysis. **A**, NA and C6 expression led to significant up-regulation of FAK and Src phosphorylation at 48 h as shown in *second lane of top two panels*. The pathway is Akt-dependent but independent of ERK activation as shown in *second lane of bottom two panels* in HEK-293 cells. Densitometry analysis ($n = 2$) of phosphorylation levels of Akt, FAK, and Src molecules in HEK-293 cells transfected with vector only and NA+C6 expression constructs are shown. Results were analyzed using paired t tests, and differences were considered significant at $p < 0.005$, $p < 0.05$, and $p < 0.01$ for P-FAK, P-Src, and P-Akt, respectively. **B**, NA expression led to significant up-regulation of FAK and Akt phosphorylation at 48 h shown in *second lane of top two panels*. P-Src and P-GSK3 β expression at 48 h after transfection is shown in *middle lane of bottom two panels*. **C**, influenza infection led to significant up-regulation of FAK and Akt phosphorylation at 48 h shown in *second lane of top three panels* in A549 cells. Total Akt and FAK antibody was used as a control (*a*). In contrast, knock down of C6 shows down-regulation of P-Akt, P-Src, and P-FAK at 24 h (*b*). Densitometry analysis of phosphorylation levels of Akt, FAK, Src molecules in infected with PR8 virus in A549 cells is shown. Results were analyzed as in **A** with values of $p < 0.04$, $p < 0.01$, $p < 0.008$, and $p < 0.02$ for P-Akt, P-FAK, P-Src, and P-GSK3 β , respectively. **C**, influenza infection led to significant up-regulation of P-Akt, P-Src, and P-FAK at 24 h, shown in *second lane of top three panels* in A549 cells. Total Akt and FAK antibody was used as a control (*a*). In contrast, knock down of C6 shows down-regulation of P-Akt, P-Src, and P-FAK at 24 h (*b*). Densitometry analysis of phosphorylation levels of Akt, FAK, Src molecules in infected with PR8 virus in A549 cells is shown. Results were analyzed as in **A** with values of $p < 0.009$, $p < 0.001$, and $p < 0.005$ for P-Akt, P-FAK, and P-Src, respectively. **D**, NHBE cells were transfected with control siRNA or C6 siRNA for 24 h. Cells were infected with PR8 (1 m.o.i.) for 24 h and harvested for the expression analysis of C6, P-Akt, P-Src, and P-Bcl-2 by Western blotting. Total Akt and Bcl-2 Western blotting was used as a control.

of Akt were reduced in cells treated with PI3K inhibitors and infected with PR8 virus (Fig. 7). PR8 infection itself activated phosphorylation of Akt in A549 and NHBE cells.

We have also assessed the viability of NHBE cells in the presence of PI3K inhibitors (supplemental Fig. S4) and our findings indicate a decrease in cell viability with LY294002 and wortmannin. PI3K inhibitors act upstream of Akt phosphorylation. Therefore, we investigated further the role of Akt phosphorylation utilizing Akt-specific inhibitors. As a control, we used Akt activator YS-49. YS-49 not only increased Akt phosphorylation (Fig. 7, *Ab* and *Bb*) but also inhibited virus-induced cell death (Fig. 7, *A* and *B*) in both A549 and NHBE cells. In contrast, Akt inhibitors Triciribine, 124005, and GSK690693 inhibited virus-induced Akt phosphorylation (Fig. 7, *Ab* and *Bb*) in A549 and NHBE cells. Akt inhibitors decreased cell viability (Fig. 7, *Ac* and *Bc*) and virus replication (Fig. 7, *Ad* and *Bd*) in PR8-infected A549 and NHBE cells. Apart from pharmacological inhibitors we also evaluated the role of Akt in survival pathway by siRNA knockdown studies. siRNA pools against Akt1,

Akt2, and Akt3 significantly reduced the Akt expression in infected or uninfected NHBE cells (Fig. 8, *Aa* and *Ba*). PR8 infection resulted in significant decrease in cell viability (Fig. 8, *Ab* and *Bb*) and viral titers in both cell lines (Fig. 8, *Ac* and *Bc*). However, despite the change in cell viability and viral titers as a result of Akt phosphorylation, we did not see significant change in plaque size (data not shown). These results suggest a role for NA-C6 in augmenting cell survival following infection with influenza virus via the Src/Akt axis.

DISCUSSION

To date, the primary role of influenza NA protein has been believed to be in the release of progeny viruses from infected cells and the subsequent spread of the virus to the surrounding uninfected cells. NA is also critical for the initiation of infection and resultant influenza pathogenesis (19, 20). During influenza infection, it triggers a host of intracellular signaling. These pathways carry out various cellular functions which usually are hijacked by the infecting virus (21). There have been limited

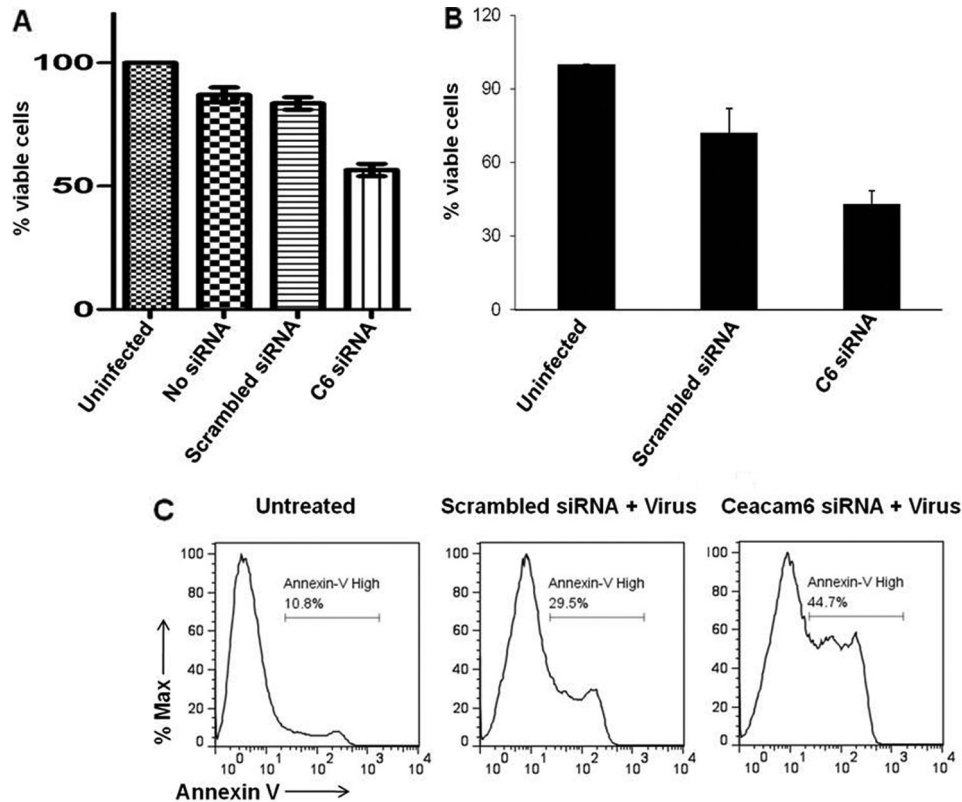


FIGURE 6. Reduction of C6 levels decreases viability of influenza A virus-infected cells. A, A549 cells were treated with siRNA (scrambled or C6-specific) followed by infection with PR8 virus at an m.o.i. of 1. Samples were examined 24 h after infection by MTT assay and the percentage of viable cells determined ($n = 2$). B, NHBE cells were treated with siRNA (control or C6-specific) followed by infection with PR8 virus at a m.o.i. of 1. Cell viability was examined 24 h after infection by MTT assay ($n = 3$). C, A549 cells were treated either with siRNA against C6 or scrambled siRNA for 48 h. Cells were infected with PR8 virus at a m.o.i. of 1. Cells were stained with Annexin-V followed by flow cytometry analysis.

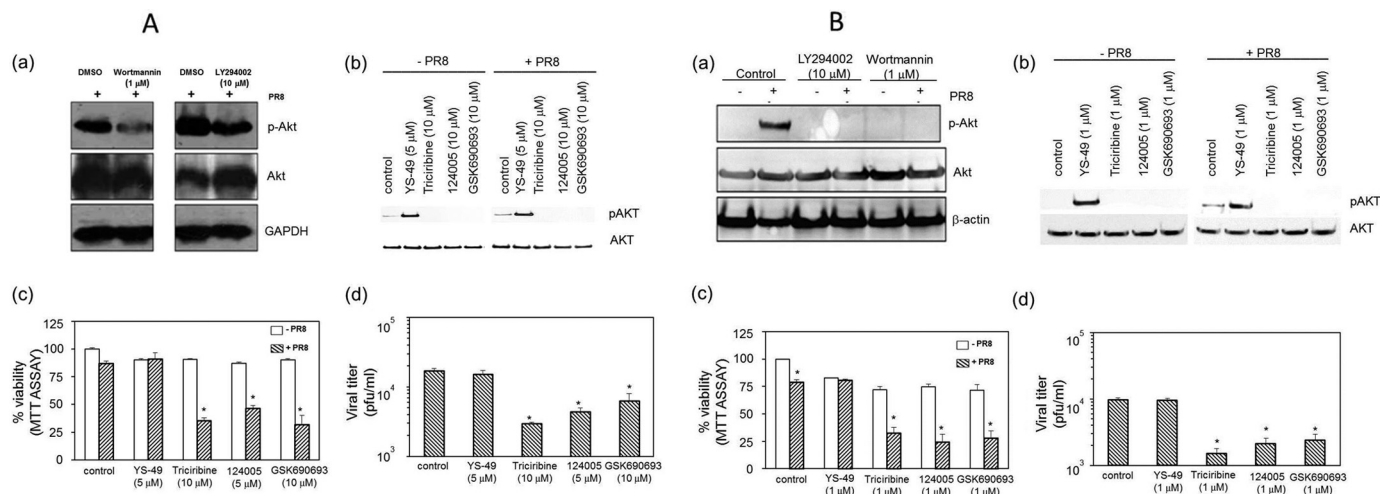


FIGURE 7. PI3K inhibitors and Akt inhibitors suppressed Akt phosphorylation and increased virus-induced cell death in A549 and NHBE cells. A and B, A549 (A) or NHBE (B) cells were infected with PR8 at m.o.i. of 1 and treated with PI3K inhibitors (LY294002 and wortmannin), Akt activator, YS-49, or Akt inhibitors, Triciribine, 124005, or GSK690693 at indicated concentrations shown. Cell lysates and supernatants were harvested 24 h after infection for the analysis of P-Akt and Akt expression by immunoblot (Aa, Ab, Ba, Bb), cell viability by MTT assay (Ac, Bc) and viral titers by plaque assay (Ad, Bd).

studies investigating a role for NA in cell signaling. Here, we demonstrate for the first time a novel function for influenza NA in the activation of Src/Akt cell survival axis via an interaction with C6. Many viruses have key proteins that have been reported to activate PI3K signaling cascades. For example, in the case of hepatitis B virus, X protein has been shown to activate cell survival signaling through the Src/PI3K (22), LMP1

protein of Epstein-Barr virus induces B cell survival. Similarly, E5 protein of papillomavirus has been shown to utilize this mechanism (23). The NS5A protein of HCV directly binds to the SH3 domain of p85 and induces PI3K/Akt-mTOR signaling to control cell survival (24). Other viruses such as SARS coronavirus (25), poliovirus (26), and dengue virus (27) also utilize the PI3K signaling pathway to their advantage.

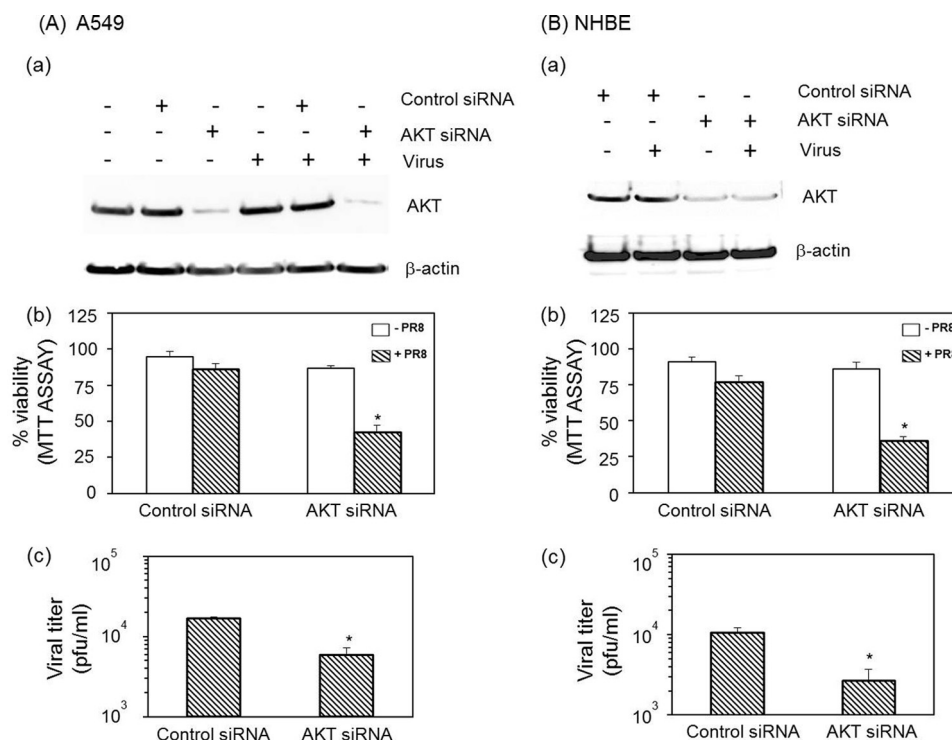


FIGURE 8. siRNA-mediated Akt knockdown impaired cell viability and influenza virus replication in A549 and NHBE cells. A549 cells (A) or (B) NHBE cells were transfected with control siRNA or siRNA specific for Akt1, Akt2, and Akt3 for 24 h and infected with PR8 (1 m.o.i.) for 24 h. Cell lysates and cell supernatants were harvested for Akt expression by immunoblot (Aa, Ba), cell viability by MTT (Ab, Bb), and viral titers by plaque assay (Ac, Bc).

C6 is a member of a family of membrane-associated glycoproteins that contain SLe^x moieties, which are involved in the binding of influenza virions to the host cell (28). CEACAM family members are localized to lipid rafts at the cell surface by either transmembrane domains or glycosylphosphatidylinositol anchors (29). These plasma membrane microdomains accumulate numerous signal transduction components and have been implicated in transmembrane signaling via Src family kinases (30). Although CEACAM family members have been shown to activate tyrosine kinase activity and play a role in inhibition of apoptosis (31, 32), the ligands that initiate these signaling pathways have not been fully elucidated.

The NA/C6 interaction described here was confirmed in a cell-free translation system and in influenza virus infected A549 and NHBE cells, where the proteins were found to co-localize in the plasma membrane. The interaction was well conserved across different subtypes of influenza viruses, including the 2009 pandemic H1N1 strain, despite significant differences in the amino acid sequences of NA.

It has previously been shown that cell adhesion-mediated FAK-Src signaling has a role in the regulation of human intestinal epithelial cell survival, with inhibition of FAK leading to increased anoikis (33). The NA/C6 interaction described here appears to activate this cell survival pathway by enhancing the phosphorylation levels of Src, FAK, Akt, and Bcl-2. The critical nature of C6 in these processes during virus infection was further established by siRNA-mediated knockdown. We have also provided evidence that indicates the involvement of Akt signaling PI3K inhibitors reduced the phosphorylation of Akt. Involvement of Akt phosphorylation in cell survival and virus replication was further confirmed using inhibitors that act directly on Akt

which decreased cell viability and viral titer in infected cells. Additional evidence in support of Akt involvement comes from the studies where we knocked down all the isoforms of Akt and observed reduced cell viability and viral titer in virus-infected cells. The phenomenon is not cell-dependent as we have obtained similar results with HEK-293, A549, and NHBE cells. In the context of viral infection, silencing C6 led to a reduction in the expression of NP and NS1 proteins as well as vRNA levels of NP (Fig. S3). Influenza virus infection has previously been shown to result in the up-regulation of expression of integrins and other neutrophil adhesion molecules (28, 34). Influenza NA has been shown to activate TGF- β (10), and CEACAM6 is a major target for Smad3-mediated TGF- β signaling (35). These observations have led us to investigate the effect of influenza virus on C6 expression levels. In this study we showed for the first time that influenza A virus-infected A549 cells show elevated C6 mRNA and protein expression. Taken together, these findings demonstrate that influenza NA protein may have additional roles in promoting cell survival during viral infection to facilitate viral replication.

Acknowledgments—We thank Dr. Yee-Joo Tan (National University of Singapore) and Dr. Wolfgang Zimmermann (Tumor Immunology Laboratory, Muenchen, Germany) for providing pIX41-NA and pRc/CMV-C6 plasmids, respectively, and Dr. Dinh Duy Khang (Institute of Biotechnology, Hanoi, Vietnam) for providing the influenza virus (Hatay isolate) cDNA and Adarsh Mayank for help with figures in the manuscript.

REFERENCES

1. Taubenberger, J. K., and Morens, D. M. (2008) The pathology of influenza virus infections. *Annu. Rev. Pathol.* 3, 499–522

2. Bouvier, N. M., and Palese, P. (2008) The biology of influenza viruses. *Vaccine* **26**, D49–53
3. Ehrhardt, C., Wolff, T., Pleschka, S., Planz, O., Beermann, W., Bode, J. G., Schmolke, M., and Ludwig, S. (2007) Influenza A virus NS1 protein activates the PI3K/Akt pathway to mediate antiapoptotic signaling responses. *J. Virol.* **81**, 3058–3067
4. Hale, B. G., and Randall, R. E. (2007) PI3K signalling during influenza A virus infections. *Biochem. Soc. Trans.* **35**, 186–187
5. Shin, Y. K., Liu, Q., Tikoo, S. K., Babiuk, L. A., and Zhou, Y. (2007) Effect of the phosphatidylinositol 3-kinase/Akt pathway on influenza A virus propagation. *J. Gen. Virol.* **88**, 942–950
6. Flory, E., Kunz, M., Scheller, C., Jassoy, C., Stauber, R., Rapp, U. R., and Ludwig, S. (2000) Influenza virus-induced NF- κ B-dependent gene expression is mediated by overexpression of viral proteins and involves oxidative radicals and activation of I κ B kinase. *J. Biol. Chem.* **275**, 8307–8314
7. Arora, D. J., and Gasse, N. (1998) Influenza virus hemagglutinin stimulates the protein kinase C activity of human polymorphonuclear leucocytes. *Arch. Virol.* **143**, 2029–2037
8. Pahl, H. L., and Baeuerle, P. A. (1995) Expression of influenza virus hemagglutinin activates transcription factor NF- κ B. *J. Virol.* **69**, 1480–1484
9. Chazal, N., and Gerlier, D. (2003) Virus entry, assembly, budding, and membrane rafts. *Microbiol. Mol. Biol. Rev.* **67**, 226–237, table of contents
10. Schultz-Cherry, S., and Hinshaw, V. S. (1996) Influenza virus neuraminidase activates latent transforming growth factor- β . *J. Virol.* **70**, 8624–8629
11. Miller, J. L., and Anders, E. M. (2003) Virus-cell interactions in the induction of type 1 interferon by influenza virus in mouse spleen cells. *J. Gen. Virol.* **84**, 193–202
12. Houde, M., and Arora, D. J. (1990) Stimulation of tumor necrosis factor secretion by purified influenza virus neuraminidase. *Cell. Immunol.* **129**, 104–111
13. Duxbury, M. S., Ito, H., Zinner, M. J., Ashley, S. W., and Whang, E. E. (2004) CEACAM6 gene silencing impairs anoikis resistance and *in vivo* metastatic ability of pancreatic adenocarcinoma cells. *Oncogene* **23**, 465–473
14. Duxbury, M. S., Ito, H., Ashley, S. W., and Whang, E. E. (2004) CEACAM6 cross-linking induces caveolin-1-dependent, Src-mediated focal adhesion kinase phosphorylation in BxPC3 pancreatic adenocarcinoma cells. *J. Biol. Chem.* **279**, 23176–23182
15. Kumar, P., Gunalan, V., Liu, B., Chow, V. T., Druce, J., Birch, C., Catton, M., Fielding, B. C., Tan, Y. J., and Lal, S. K. (2007) The nonstructural protein 8 (nsp8) of the SARS coronavirus interacts with its ORF6 accessory protein. *Virology* **366**, 293–303
16. Ratra, R., Kar-Roy, A., and Lal, S. K. (2009) ORF3 protein of hepatitis E virus interacts with the β chain of fibrinogen resulting in decreased fibrinogen secretion from HuH-7 cells. *J. Gen. Virol.* **90**, 1359–1370
17. Duxbury, M. S., Ito, H., Benoit, E., Waseem, T., Ashley, S. W., and Whang, E. E. (2004) A novel role for carcinoembryonic antigen-related cell adhesion molecule 6 as a determinant of gemcitabine chemoresistance in pancreatic adenocarcinoma cells. *Cancer Res.* **64**, 3987–3993
18. Duxbury, M. S., Ito, H., Benoit, E., Zinner, M. J., Ashley, S. W., and Whang, E. E. (2004) Overexpression of CEACAM6 promotes insulin-like growth factor I-induced pancreatic adenocarcinoma cellular invasiveness. *Oncogene* **23**, 5834–5842
19. Bhatia, A., and Kast, R. E. (2007) How influenza's neuraminidase promotes virulence and creates localized lung mucosa immunodeficiency. *Cell Mol. Biol. Lett.* **12**, 111–119
20. Matrosovich, M. N., Matrosovich, T. Y., Gray, T., Roberts, N. A., and Klenk, H. D. (2004) Neuraminidase is important for the initiation of influenza virus infection in human airway epithelium. *J. Virol.* **78**, 12665–12667
21. Gaur, P., Munjhal, A., and Lal, S. K. (2011) Influenza virus and cell signaling pathways. *Med. Sci. Monit.* **17**, RA148–154
22. Shih, W. L., Kuo, M. L., Chuang, S. E., Cheng, A. L., and Doong, S. L. (2003) Hepatitis B virus X protein activates a survival signaling by linking SRC to phosphatidylinositol 3-kinase. *J. Biol. Chem.* **278**, 31807–31813
23. Cooray, S. (2004) The pivotal role of phosphatidylinositol 3-kinase/Akt signal transduction in virus survival. *J. Gen. Virol.* **85**, 1065–1076
24. Mannová, P., and Beretta, L. (2005) Activation of the N-Ras-PI3K-Akt-mTOR pathway by hepatitis C virus: control of cell survival and viral replication. *J. Virol.* **79**, 8742–8749
25. Mizutani, T., Fukushi, S., Saijo, M., Kurane, I., and Morikawa, S. (2004) Importance of Akt signaling pathway for apoptosis in SARS-CoV-infected Vero E6 cells. *Virology* **327**, 169–174
26. Autret, A., Martin-Latil, S., Brisac, C., Mousson, L., Colbère-Garapin, F., and Blondel, B. (2008) Early phosphatidylinositol 3-kinase/Akt pathway activation limits poliovirus-induced JNK-mediated cell death. *J. Virol.* **82**, 3796–3802
27. Lee, C. J., Liao, C. L., and Lin, Y. L. (2005) Flavivirus activates phosphatidylinositol 3-kinase signaling to block caspase-dependent apoptotic cell death at the early stage of virus infection. *J. Virol.* **79**, 8388–8399
28. Hartshorn, K. L., and White, M. R. (1999) Influenza A virus up-regulates neutrophil adhesion molecules and adhesion to biological surfaces. *J. Leukoc. Biol.* **65**, 614–622
29. Kuespert, K., Pils, S., and Hauck, C. R. (2006) CEACAMs: their role in physiology and pathophysiology. *Curr. Opin. Cell Biol.* **18**, 565–571
30. Kasahara, K., Watanabe, K., Kozutsumi, Y., Oohira, A., Yamamoto, T., and Sanai, Y. (2002) Association of GPI-anchored protein TAG-1 with src-family kinase Lyn in lipid rafts of cerebellar granule cells. *Neurochem. Res.* **27**, 823–829
31. Kirshner, J., Chen, C. J., Liu, P., Huang, J., and Shively, J. E. (2003) CEACAM1–4S, a cell-cell adhesion molecule, mediates apoptosis and reverts mammary carcinoma cells to a normal morphogenic phenotype in a 3D culture. *Proc. Natl. Acad. Sci. U.S.A.* **100**, 521–526
32. Najjar, S. M. (2002) Regulation of insulin action by CEACAM1. *Trends Endocrinol. Metab.* **13**, 240–245
33. Bouchard, V., Demers, M. J., Thibodeau, S., Laquerre, V., Fujita, N., Tsuruo, T., Beaulieu, J. F., Gauthier, R., Vézina, A., Villeneuve, L., and Vachon, P. H. (2007) Fak/Src signaling in human intestinal epithelial cell survival and anoikis: differentiation state-specific uncoupling with the PI3-K/Akt-1 and MEK/Erk pathways. *J. Cell Physiol.* **212**, 717–728
34. Ducker, T. P., and Skubitz, K. M. (1992) Subcellular localization of CD66, CD67, and NCA in human neutrophils. *J. Leukoc. Biol.* **52**, 11–16
35. Han, S. U., Kwak, T. H., Her, K. H., Cho, Y. H., Choi, C., Lee, H. J., Hong, S., Park, Y. S., Kim, Y. S., Kim, T. A., Kim, S. J. (2008) CEACAM5 and CEACAM6 are major target genes for Smad3-mediated TGF- β signaling. *Oncogene* **27**, 675–683